

# Regioselective Electrosynthesis of Rare 1,2,3,16-Functionalized [60]Fullerene Derivatives\*\*

Yang Xiao, San-E Zhu, Ding-Jia Liu, Mitsuaki Suzuki, Xing Lu,\* and Guan-Wu Wang\*

**Abstract:** Fullerene derivatives with different addition patterns exhibit different physical, chemical, and biological properties, which are important for fullerene applications. Novel and rare 1,2,3,16-functionalized [60]fullerene derivatives having a five-membered heterocycle fused to a [5,6]-junction were obtained with high regioselectivity by electrochemical derivatization of a [60]fulleroindoline. The product structures were determined by spectroscopic data and single-crystal X-ray analysis. The obtained high regioselectivity was rationalized using theoretical calculations.

Recently, multiple addition reactions of fullerenes have attracted attention because of the potential applications of functionalized fullerenes in many different areas such as materials and biological science.<sup>[1]</sup> However, owing to the formation of various regioisomers in the preparation of fullerene multiadducts, regiocontrol of the multiple addition reactions has become one of the major challenges.<sup>[2,3]</sup> A mixture of up to eight regioisomeric bis(adducts) of [60]fullerene (C<sub>60</sub>), that is, *cis*-1, *cis*-2, *cis*-3, *e*, *trans*-1, *trans*-2, *trans*-3, and *trans*-4 isomers, by cycloaddition reactions can be generated.<sup>[2]</sup> Elegant approaches to achieve high regioselectivity are the template-mediated and tether-directed multifunctionalizations of fullerenes developed by the groups of Hirsch and Diederich, respectively.<sup>[4]</sup> As for tetrafunctionalized C<sub>60</sub> derivatives containing noncyclic addends, the reported common regioisomers are 1,2,3,4-isomers (**A**),<sup>[5]</sup> 1,4,11,15-isomers (**B**),<sup>[6]</sup> and 1,2,4,15-isomers (**C**; Figure 1), which can be synthesized by either chemical or electrochemical methods. In contrast, the 1,2,3,16-isomers (**D**) are

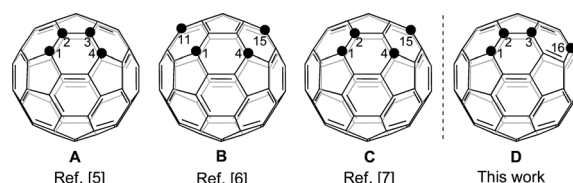


Figure 1. Addition patterns of tetrafunctionalized C<sub>60</sub> derivatives.

scarce and much less investigated.<sup>[8]</sup> Rubin and co-workers reported the synthesis of bicyclic octahydroquinolino-1,2,3,4-tetrahydrofullerenes by the tandem nucleophilic addition/Diels–Alder reaction of *N*-butadienyl *N,O*-ketene silyl acetals with C<sub>60</sub>, and the obtained 1,2,3,4-adducts were then transformed into 1,2,3,16-adducts by deprotonation with subsequent hydroxylation or alkylation.<sup>[8a]</sup> Alternatively, nucleophilic addition to C<sub>60</sub> by the Grignard reagent generated from 2-(bromoethyl)-1,3-dioxolane afforded a 1,2-organodihydrofullerene acetal, which was then deprotonated, methylated, and hydrolyzed to give a 1,4-organodihydrofullerene aldehyde. Subsequent condensation with aniline and then intramolecular Diels–Alder reaction took place at the neighboring C=C bond on the fullerene surface and then aromatization provided the final 1,2,3,16-adduct.<sup>[8b]</sup> Although fullerene derivatives with structures of types **A** and **C** have been successfully obtained by electrosynthesis, the synthesis of the rare type **D** structure has never been realized electrochemically. Herein, we disclose that efficient and straightforward synthesis of several 1,2,3,16-adducts can be achieved by treating the electrochemically generated dianion of a C<sub>60</sub>-fused indoline derivative with either benzyl bromide or ethyl bromoacetate. Importantly, either one or two CH<sub>2</sub>Ph or CH<sub>2</sub>CO<sub>2</sub>Et moieties can be selectively introduced onto the fullerene skeleton by rational control of the reaction conditions, thus demonstrating the practicality and diversity of the current protocol.

The employed [60]fulleroindoline **1** (for structure see Scheme 1) was synthesized according to our previous procedure.<sup>[9]</sup> The cyclic voltammogram (CV) of **1** in *o*-dichlorobenzene (ODCB; Figure 2a) shows that the first redox is a reversible one-electron transfer process with an *E*<sub>1/2</sub> of −0.56 V versus a saturated calomel electrode, whereas the second redox is chemically irreversible on the CV timescale, as evidenced by the appearance of decreased anodic current in the reverse scan.<sup>[5c,10,11]</sup> This result indicates that a heterolytic cleavage of the C<sub>60</sub>–N bond likely occurs after **1** accepts two electrons (Scheme 1).<sup>[5c,11]</sup> This process was further confirmed by the *in situ* visible/near-infrared (Vis/NIR) study of dianionic **1** obtained by controlled potential electrolysis (CPE) at −1.1 V. The Vis/NIR spectrum of **1**<sup>2−</sup>

[\*] Y. Xiao, Dr. S.-E. Zhu, D.-J. Liu, Prof. Dr. G.-W. Wang  
Hefei National Laboratory for Physical Sciences at Microscale  
CAS Key Laboratory of Soft Matter Chemistry, and Department of  
Chemistry, University of Science and Technology of China  
Hefei, Anhui 230026 (P. R. China)  
E-mail: gwang@ustc.edu.cn

Dr. M. Suzuki, Prof. Dr. X. Lu  
State Key Laboratory of Materials Processing and Die & Mould  
Technology, School of Materials Science and Engineering  
Huazhong University of Science and Technology (HUST)  
Wuhan, Hubei 430074 (P. R. China)  
E-mail: lux@hust.edu.cn

[\*\*] We are grateful for financial support from the National Natural Science Foundation of China (21132007, 21171061) and the Specialized Research Fund for the Doctoral Program of Higher Education (20123402130011). The assistance in the Vis/NIR spectral measurement by Prof. Xiang Gao is cordially acknowledged.



Supporting information for this article is available on the WWW under <http://dx.doi.org/10.1002/ange.201310565>.

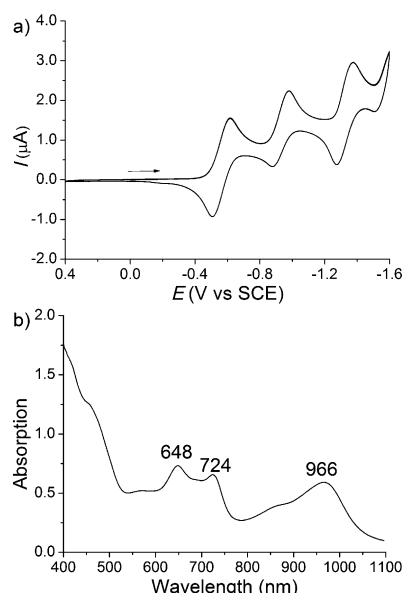
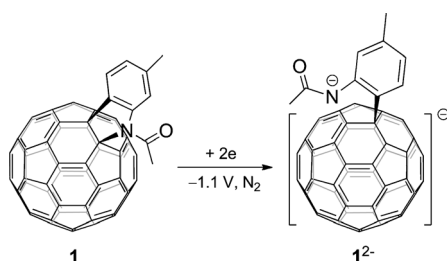


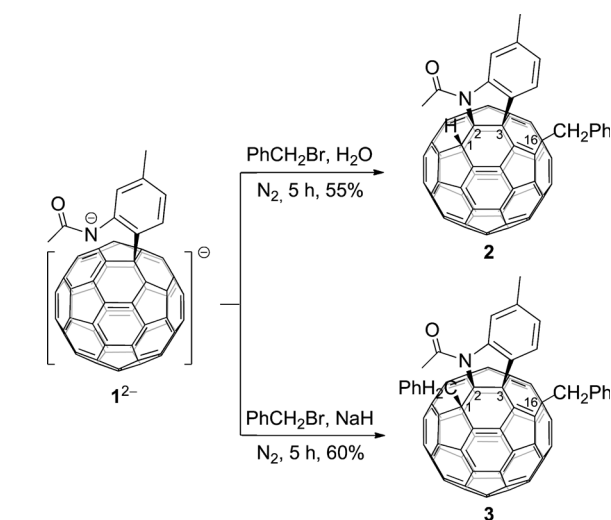
**Figure 2.** a) Cyclic voltammogram of **1** ( $1.0 \times 10^{-3}$  M) recorded in ODCB containing 0.1 M tetra-*n*-butylammonium perchlorate (TBAP) starting from 0.0 V toward the negative potential at a scan rate of  $20 \text{ mVs}^{-1}$ . b) In situ Vis/NIR spectrum of  $1^{2-}$  in ODCB ( $1.8 \times 10^{-3}$  M).



**Scheme 1.** Formation of  $1^{2-}$  involving the  $\text{C}_{60}$ -N bond cleavage upon acceptance of two electrons via CPE at  $-1.1 \text{ V}$ .

(Figure 2b) shows strong absorption bands at  $\lambda = 966$ ,  $724$  and  $648 \text{ nm}$ , which are in excellent agreement with those of the singly bonded dianions of a [60]fulleropyrazole ( $\lambda = 963$ ,  $710$  and  $645 \text{ nm}$ )<sup>[7e]</sup> and a [60]fullerosultone ( $\lambda = 983$  and  $648 \text{ nm}$ ).<sup>[11]</sup>

The unique ring-opened structure of  $1^{2-}$  makes it a perfect building block in electrosynthesis. When  $1^{2-}$  was treated with 1.5 equivalents of  $\text{PhCH}_2\text{Br}$  for 5 hours at ambient temperature, the product **2**, with a 1,2,3,16-addition pattern, was obtained exclusively in 55% yield (Scheme 2). Apparently, a hydrogen and a benzyl group were regioselectively added to the fullerene skeleton at C1 and C16, respectively, accompanied by the migration of the indoline moiety from a [6,6]-junction to a [5,6]-junction on the fullerene surface. As has been demonstrated previously by Gao et al., the most likely source of the fullerenyl proton in **2** is the water residue in ODCB, and it is extremely difficult to completely remove it from the organic solvent even after a strict drying treatment.<sup>[12]</sup> However, when a tenfold excess of water was added, the yield of **2** was decreased slightly to 51%, thus indicating that the water contained in the solvent was enough for the reaction and that too much water was unfavorable. Intriguingly,

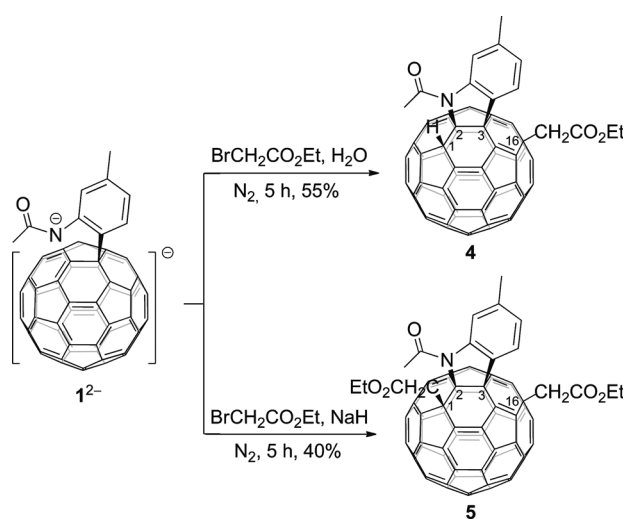


**Scheme 2.** Reaction of  $1^{2-}$  with benzyl bromide under different reaction conditions.

when NaH was added to remove the trace amount of water present in the system and a large excess of  $\text{PhCH}_2\text{Br}$  was used, another 1,2,3,16-adduct with two  $\text{PhCH}_2$  groups could be selectively generated. When  $1^{2-}$  was allowed to react with NaH and benzyl bromide (1:50:50) for 5 hours, **3** was formed in 60% yield (Scheme 2).

The reaction could be extended to other substrates. We then employed ethyl bromoacetate as another representative electrophile. Similarly, the reaction of  $1^{2-}$  with ethyl bromoacetate (1:1.5) afforded **4** in 55% yield, while treatment of  $1^{2-}$  with NaH and ethyl bromoacetate (1:100:100) provided **5** in 40% yield (Scheme 3).

Products **2–5** were characterized by MALDI-TOF MS,  $^1\text{H}$  NMR,  $^{13}\text{C}$  NMR, FT-IR, and UV/Vis spectroscopy, and **2** was further identified by single-crystal X-ray crystallography. The mass spectra of **2–5** show corresponding  $[M+\text{Na}]^+$  ion peaks. In the  $^1\text{H}$  NMR spectrum of **2**, besides the signals from



**Scheme 3.** Reaction of  $1^{2-}$  with ethyl bromoacetate under different reaction conditions.

the aromatic moiety, a singlet for the fullerenyl proton at  $\delta = 5.99$  ppm and an AB quartet at  $\delta = 4.43$  and 4.21 ppm with  $J = 13.2$  Hz, for the protons of the methylene group bonded to the fullerene cage, are observed.<sup>[5c]</sup> Similarly, the  $^1\text{H}$  NMR spectrum of **4** shows a singlet at  $\delta = 5.98$  ppm for the fullerenyl proton and an AB quartet at  $\delta = 4.06$  and 3.89 ppm with  $J = 14.6$  Hz for the methylene protons. Compared to the  $^1\text{H}$  NMR spectra of **2** and **4**, the absence of the fullerenyl proton signal and the appearance of an additional AB quartet for the methylene protons of  $\text{CH}_2\text{-C}_{60}$  in the  $^1\text{H}$  NMR spectra of **3** and **5** suggest that the fullerenyl proton is substituted by an additional  $\text{RCH}_2$  ( $\text{R} = \text{Ph}$ ,  $\text{CO}_2\text{Et}$ ) group. The  $^{13}\text{C}$  NMR spectra of **2–5** exhibit more than 51 peaks in the range of  $\delta = 157\text{--}133$  ppm for the 56  $\text{sp}^2$ -carbon atoms of the fullerene cage, and four peaks between  $\delta = 89\text{--}52$  ppm for the four  $\text{sp}^3$ -carbon atoms of the fullerene skeleton, all of which are consistent with their  $C_1$  symmetry. The UV/Vis spectrum of **2**, distinct from that of the starting material **1**, has three major absorption bands at  $\lambda = 253$ , 316, and 403 nm, along with two weak absorption bands at  $\lambda = 701$  and 747.5 nm, similar to those of 1,2,3,16-functionalized fullerenes in the literature.<sup>[8]</sup> The fact that the UV/Vis spectra of **3–5** are nearly identical to that of **2**, indicates that they are also 1,2,3,16-adducts (see Figure S1 in the Supporting Information).

Single crystals of **2** were obtained by slow evaporation of its toluene solution at room temperature. As a consequence of the inherent chirality possessed by the 1,2,3,16-configuration, the crystal structure contains a pair of enantiomers, but in unequal amounts. The two disordered  $\text{C}_{60}$  cages are in a ratio of 0.58:0.42, although the addends and a majority of the cage carbon atoms overlap. Similar situations related to the orientational disorder are encountered in many fullerene crystals.<sup>[13]</sup> The structure of the major enantiomer (Figure 3) reveals clearly that a heterocycle is bonded to  $\text{C}_{60}$  through a N

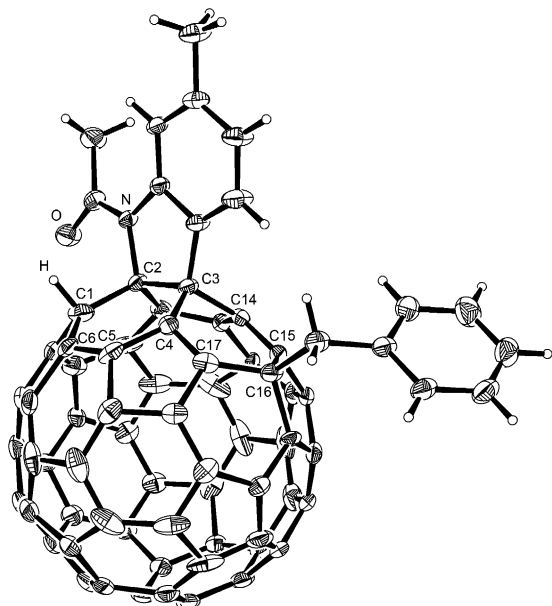


**Figure 3.** ORTEP diagram for the major enantiomer (0.58 occupancy) of **2** with thermal ellipsoids shown at 20% probability. The minor enantiomer and the toluene molecule are omitted for clarity.

and a  $\text{C}_{\text{aryl}}$  at the C2 and C3 positions, respectively, and that a hydrogen atom is attached to C1. As for the benzyl group, it is located at the C16 position, distant from the other three addends. The four functionalized carbon atoms of the fullerene cage are uplifted from the spherical surface notably because of their  $\text{sp}^3$  character. The bond lengths for C1–C2, C3–C4, C4–C5, C1–C6, C3–C14, C15–C16, and C16–C17 are 1.544(7) Å, 1.504(7) Å, 1.465(13) Å, 1.494(11) Å, 1.523(7) Å, 1.516(8) Å, and 1.513(8) Å, respectively, and are within the range of typical C–C bond lengths. In comparison, the bond length for C2–C3 is 1.620(7) Å, which is remarkably elongated with respect to a C–C bond,<sup>[5b,13]</sup> whereas C5–C6, C4–C17, and C14–C15 have bond lengths of 1.374(10) Å, 1.356(7) Å, and 1.369(7) Å, respectively, thus possessing double bond character. To our knowledge, this is the first single-crystal structure for 1,2,3,16-adducts of  $\text{C}_{60}$ .

To gain insight into the regioselective formation of the 1,2,3,16-adducts, density functional theory calculations at the B3LYP/6-31G\* level of theory were performed. Figure 4 shows the partial natural bond orbital (NBO) charge distri-

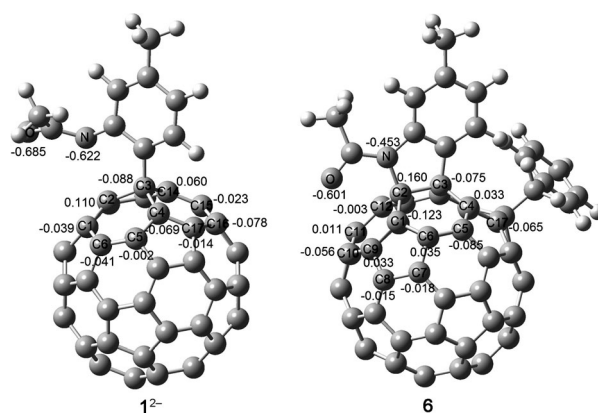


**Figure 4.** Partial NBO charge distributions of  $1^{2-}$  and **6**.

bution of the optimized  $1^{2-}$ , which possesses a ring-opened structure from a  $\text{C}_{60}\text{-N}$  bond rupture. C16 (−0.078) and C4 (−0.069)<sup>[14]</sup> are the two most negatively charged carbon atoms among the nonfunctionalized  $\text{C}_{60}$  carbon atoms, and are more prone to react with an electrophile. The preferred reaction pathway would be governed by both the electron density of the attacking carbon atom and steric hindrance encountered in the forming species. Therefore, the regioselectivity is dependent on the size of the addends and the stability of the resulting intermediates.<sup>[5c,d]</sup> In the optimized structure of  $1^{2-}$ , the nitrogen atom locates above C2 with a distance of merely 2.532 Å. This distance is so short that the two nearby atoms tend to bond together immediately in the subsequent reaction process to form a heterocycle fused with a [5,6]-junction. Taking the reaction of  $1^{2-}$  with benzyl bromide as an example, the most likely intermediate is either **6** or **7**, after the addition of the benzyl group to  $1^{2-}$ , and subsequent ring-closure process. Compared to **7**, **6** has a double bond in a five-membered ring, which is energetically unfavorable.<sup>[6a,8a]</sup> Nevertheless, this unfavorable energy increase would be compensated by a decrease in steric hindrance between the

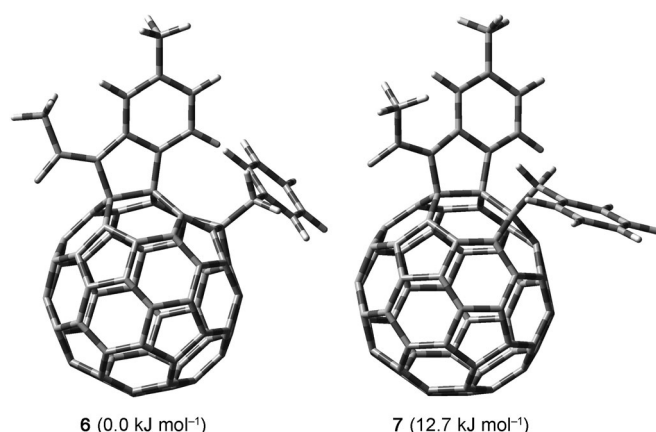


Figure 5. Relative energies of optimized **6** and **7**.

bulky benzyl group and the existing aryl appendage when it is located in the *para* position. As a consequence, **6** should be preferably formed as it is more stable than **7** by 12.7 kJ mol<sup>−1</sup> (Figure 5). The NBO charge distribution of **6** (Figure 4) shows that C1 carries a much greater negative charge (−0.123) than other nonfunctionalized fullerene carbon atoms, and should be the most easily protonated. However, the electron densities at C5, C10, and C17 are also relatively high, and thus these carbon atoms could also be potential reaction sites. To better understand the regioselective formation of **2**, further calculations on the stability of **2** and the regioisomers **2a–c** (generated by protonation on C5, C10, and C17 atoms, respectively) were carried out. The calculation results indicate that **2** is more stable than **2a–c** by at least 24.8 kJ mol<sup>−1</sup> (see Figure S4), thus making it clear that the protonation should be preferred at C1. Similar to **2**, **3** is more stable than its regioisomers **3a–c** by more than 15.1 kJ mol<sup>−1</sup> (see Figure S5). The above computational results corroborate strongly with our experimental results, thus explaining why products with the 1,2,3,16-configuration can be regioselectively generated.

In summary, we have achieved the efficient and regioselective syntheses of the rare 1,2,3,16-adducts by the reaction of the dianionic **1**<sup>2−</sup>, which is formed by the electroreduction of **1**, with benzyl bromide or ethyl bromoacetate. Intriguingly, either one or two CH<sub>2</sub>Ph or CH<sub>2</sub>CO<sub>2</sub>Et groups are selectively introduced onto the fullerene surface in the absence or presence of sodium hydride. After receiving two electrons, **1** undergoes a C<sub>60</sub>–N bond cleavage to give a ring-opened intermediate **1**<sup>2−</sup>, which cyclizes to provide a heterocycle bonded to a [5,6]-junction from the original [6,6]-junction upon the addition of either a CH<sub>2</sub>Ph or a CH<sub>2</sub>CO<sub>2</sub>Et group at C16. The structural assignment for the products **2–5** as corresponding 1,2,3,16-adducts is unequivocally established by single-crystal X-ray crystallography. The observed regioselectivity is controlled by both charge distribution and steric factors, as supported by the computational results. It is expected that further chemical or electrochemical functionalizations of the 1,2,3,16-adducts would provide new fullerene derivatives with novel addition patterns and different properties.

## Experimental Section

Electrochemical synthesis of **1**: 25.6 mg (0.030 mmol) of **1** was electroreduced by CPE at −1.10 V vs SCE in 16.5 mL of ODCB solution containing 0.1 M TBAP under nitrogen at room temperature. The potentiostat was turned off when the theoretical number of coulombs required for full conversion of **1** into **1**<sup>2−</sup> was reached. For the preparation of **2** and **4**, 0.045 mmol of benzyl bromide or ethyl bromoacetate were added to the solution of **1**<sup>2−</sup>, and the reaction was stirred for 5 h. The reaction mixture was then filtered through a silica gel plug to remove TBAP. After evaporation in vacuo, the residue was separated on a silica gel column with CS<sub>2</sub>/CH<sub>2</sub>Cl<sub>2</sub> (3:1) as the eluent and washed three times with acetone to afford **2/4**. For the preparation of **3** and **5**, NaH (57–63 % oil dispersion, 1.500 mmol for **3** or 3.000 mmol for **5**) and benzyl bromide (1.500 mmol) or ethyl bromoacetate (3.000 mmol) were sequentially added to the solution of **1**<sup>2−</sup>. The reaction was stirred for 5 h. The same workup procedure as for **2/4** afforded **3/5**.

Crystal data for C<sub>76</sub>H<sub>17</sub>NO·C<sub>7</sub>H<sub>8</sub> (**2**·C<sub>7</sub>H<sub>8</sub>): Crystals grown by slow evaporation of a saturated solution in toluene at room temperature. Black blocks, 0.32 × 0.24 × 0.20 mm<sup>3</sup>; orthorhombic, space group *Pbca*, *a* = 14.8117(3), *b* = 22.3284(6), *c* = 27.3697(7) Å, *a* = 90.00, *b* = 90.00, *c* = 90.00°, *V* = 9051.8(4) Å<sup>3</sup>, *λ* = 1.54184 Å, *Z* = 8; *ρ*<sub>calc</sub> = 1.544 mg m<sup>−3</sup>; *μ* = 0.703 mm<sup>−1</sup>, *T* = 288(2) K; Gemini S Ultra CCD detector; *ω* scans, 2 $\theta$ <sub>max</sub> = 132.06°; 22 559 reflections collected; 7737 independent reflections (*R*<sub>int</sub> = 0.0581); Direct methods solution (SHELXS97);<sup>[15]</sup> full-matrix least-squares based on *F*<sup>2</sup> (SHELXL97);<sup>[15]</sup> *R*<sub>1</sub> = 0.1374, *wR*<sub>2</sub> = 0.2897 for all data; conventional *R*<sub>1</sub> = 0.0924 computed for 4767 observed data (*I* > 2 $\sigma$ (*I*)) with 878 parameters and 134 restraints. CCDC 974718 contains the supplementary crystallographic data for this paper. These data can be obtained free of charge from The Cambridge Crystallographic Data Centre via [www.ccdc.cam.ac.uk/data\\_request/cif](http://www.ccdc.cam.ac.uk/data_request/cif).

Calculations were performed with the Gaussian09 program<sup>[16]</sup> at the B3LYP/6-31G\* level.

Received: December 5, 2013

Published online: February 5, 2014

**Keywords:** electrochemistry · fullerenes · rearrangement · regioselectivity

- [1] For selected reviews, see: a) F. Diederich, M. Gómez-López, *Chem. Soc. Rev.* **1999**, 28, 263–277; b) E. Nakamura, H. Isobe, *Acc. Chem. Res.* **2003**, 36, 807–815; c) C.-Z. Li, H.-L. Yip, A. K.-Y. Jen, *J. Mater. Chem.* **2012**, 22, 4161–4177.
- [2] For examples on bis(adduct)s of C<sub>60</sub>, see: a) A. Hirsch, I. Lamparth, H. R. Karfunkel, *Angew. Chem.* **1994**, 106, 453–455; *Angew. Chem. Int. Ed. Engl.* **1994**, 33, 437–438; b) G. Schick, A. Hirsch, H. Mauser, T. Clark, *Chem. Eur. J.* **1996**, 2, 935–943; c) Q. Lu, D. I. Schuster, S. R. Wilson, *J. Org. Chem.* **1996**, 61, 4764–4768; d) F. Djojo, A. Herzog, I. Lamparth, F. Hampel, A. Hirsch, *Chem. Eur. J.* **1996**, 2, 1537–1547; e) Y. Nakamura, N. Takano, T. Nishimura, E. Yashima, M. Sato, T. Kudo, J. Nishimura, *Org. Lett.* **2001**, 3, 1193–1196; f) K. Kordatos, S. Bosi, T. Da Ros, A. Zambon, V. Lucchini, M. Prato, *J. Org. Chem.* **2001**, 66, 2802–2808.
- [3] For elegant work on tris(adduct)s of C<sub>60</sub>, see: S. Marchesan, T. Da Ros, M. Prato, *J. Org. Chem.* **2005**, 70, 4706–4713.
- [4] For a review, see: F. Diederich, R. Kessinger, *Acc. Chem. Res.* **1999**, 32, 537–545.
- [5] For some representative examples on type **A** derivatives, see: a) A. W. Jensen, A. Khong, M. Saunders, S. R. Wilson, D. I. Schuster, *J. Am. Chem. Soc.* **1997**, 119, 7303–7307; b) M. Yamada, W. B. Schweizer, F. Schoenebeck, F. Diederich, *Chem. Commun.* **2010**, 46, 5334–5336; c) W.-W. Yang, Z.-J. Li,

- F.-F. Li, X. Gao, *J. Org. Chem.* **2011**, 76, 1384–1389; d) C.-L. He, R. Liu, D.-D. Li, S.-E. Zhu, G.-W. Wang, *Org. Lett.* **2013**, 15, 1532–1535.
- [6] For some representative examples on type **B** derivatives, see: a) G. Schick, K.-D. Kampe, A. Hirsch, *J. Chem. Soc. Chem. Commun.* **1995**, 2023–2024; b) Y. Murata, M. Shiro, K. Komatsu, *J. Am. Chem. Soc.* **1997**, 119, 8117–8118; c) L.-L. Deng, S.-L. Xie, C. Yuan, R.-F. Liu, J. Feng, L.-C. Sun, X. Lu, S.-Y. Xie, R.-B. Huang, L.-S. Zheng, *Sol. Energy Mater. Sol. Cells* **2013**, 111, 193–199; d) T. T. Clikeman, S. H. M. Deng, S. Avdoshenko, X.-B. Wang, A. A. Popov, S. H. Strauss, O. V. Boltalina, *Chem. Eur. J.* **2013**, 19, 15404–15409.
- [7] For some representative examples on type **C** derivatives, see: a) K. M. Kadish, X. Gao, E. V. Caemelbecke, T. Suenobu, S. Fukuzumi, *J. Am. Chem. Soc.* **2000**, 122, 563–570; b) Y. Matsuo, A. Iwashita, Y. Abe, C.-Z. Li, K. Matsuo, M. Hashiguchi, E. Nakamura, *J. Am. Chem. Soc.* **2008**, 130, 15429–15436; c) M. Nambo, A. Wakamiya, S. Yamaguchi, K. Itami, *J. Am. Chem. Soc.* **2009**, 131, 15112–15113; d) I. V. Kuvychko, A. V. Streletskii, N. B. Shustova, K. Seppelt, T. Drewello, A. A. Popov, S. H. Strauss, O. V. Boltalina, *J. Am. Chem. Soc.* **2010**, 132, 6443–6462; e) W.-W. Chang, Z.-J. Li, W.-W. Yang, X. Gao, *Org. Lett.* **2012**, 14, 2386–2389.
- [8] a) Y. Rubin, P. S. Ganapathi, A. Franz, Y.-Z. An, W. Qian, R. Neier, *Chem. Eur. J.* **1999**, 5, 3162–3184; b) E. Champeil, C. Crean, C. Larraya, G. Pescitelli, G. Proni, L. Ghosez, *Tetrahedron* **2008**, 64, 10319–10330.
- [9] B. Zhu, G.-W. Wang, *Org. Lett.* **2009**, 11, 4334–4337.
- [10] a) S. Sergeyev, M. Schär, P. Seiler, O. Lukyanova, L. Eche-goyen, F. Diederich, *Chem. Eur. J.* **2005**, 11, 2284–2294.
- [11] R. Liu, F. Li, Y. Xiao, D.-D. Li, C.-L. He, W.-W. Yang, X. Gao, G.-W. Wang, *J. Org. Chem.* **2013**, 78, 7093–7099.
- [12] W.-W. Yang, Z.-J. Li, X. Gao, *J. Org. Chem.* **2010**, 75, 4086–4094.
- [13] For examples, see: a) G. P. Miller, M. C. Tetreau, M. M. Olmstead, P. A. Lord, A. L. Balch, *Chem. Commun.* **2001**, 1758–1759; b) Y. Murata, M. Suzuki, Y. Rubin, K. Komatsu, *Bull. Chem. Soc. Jpn.* **2003**, 76, 1669–1672.
- [14] The numbering of the carbon atoms on the fullerene skeleton is the same as that in the 1,2,3,16-adducts so as to easily correlate the atoms from intermediates to products.
- [15] G. M. Sheldrick, *Acta Crystallogr. Sect. A* **2008**, 64, 112–122.
- [16] Gaussian09 (Revision B.01), M. J. Frisch, et al., Gaussian Inc., Wallingford, CT, **2010**.